Supplementary Materials

High-performing and stable semiconductor yttrium-doped gadolinium electrolyte for low-temperature solid oxide fuel cells

Junjiao Li[a#], Muhammad Yousaf[b#], Muhammad Akbar[c], Asma Noor[d], Hu Enyi[b], M.A.K Yousaf Shah[b], Qadeer Akbar[e], Naveed Mushtaq[b], Yuzheng Lu[f*]

[a.] *Department of Electronic and Engineering, Nanjing Vocational Institute of Mechatronic Technology, Nanjing 211306, P.R. China*
[b.] *Jiangsu Provincial Key Laboratory of Solar Energy Science and Technology/ Energy Storage Joint Research Center, School of Energy and Environment, Southeast University, Nanjing 210096, China.*
[c.] *Key Laboratory of Ferro and Piezoelectric Materials and Devices of Hubei Province, Faculty of Physics and Electronic Science, Hubei University, Wuhan, Hubei, 430062, PR China*
[d.] *Shenzhen Key Laboratory of Laser Engineering, Guangdong Provincial Key Laboratory of Micro/Nano Optomechatronics Engineering, College of Physics and Optoelectronic Engineering, Shenzhen University, Shenzhen 518060, China*
[e.] *Department of Physics, Ajou University Swaan, Korea*
[f.] *College of Electronic and Engineering, Nanjing Xiaozhuang University, Nanjing 211171, P.R. China*
Junjiao Li, Muhammad Yousaf contributed equally to this work.

2.1 Material synthesis.

YDG powder was prepared by the co-precipitation method. Gd $(NO_3)_3.9H_2O$ (99.95%, Sigma Aldric) and $Y(NO_3)_2.6H_2O$ (99.1%, Aladdin), were dissolved into deionized water separately and kept under stirring for one and half hours. Na_2CO_3 was used as a precipitating agent, dissolved in a separate solution and added into YDG dropwise to form precipitates. The YGD solution to Na_2CO_3 molar ratio was held constant at 1:1, followed by stirring the solution for 5 hours. Filtered the solution and put the precursor in the oven at 120 ℃ for 24 hours. After drying, the precursor was calcined at 850 ℃ for 5 hours to get fine nanoparticles.

2.2 Device fabrication

$Ni0_{.8}Co_{0.15}Al_{0.5}LiO_x$ (NCAL) purchased from Tianjin Bamo Sci. &Tech. Joint Stock Ltd, China) was used as a symmetrical electrode with the electrolyte YDG. NCAL slurry was made by mixing NCAL and terpineol. The slurry was then painted on Ni-foam. After painting NCAL slurry on Ni foam, it was dried for 25 minutes at 130 °C. in the oven. Based on the prepared materials, YDG electrolyte

based SOFCs were formed by compacting the YDG powder between two pieces of NCAL-Ni electrodes circumferentially for 2 minutes under a pressure of 200 MPa. The resulting Ni-NCAL/YDG /NCAL-Ni pellet has a diameter of 13 mm and an active area of 0.64 cm^{-2}. YDG-5 and YDG-15 electrolyte based SOFCs were also constructed using the same procedure.

2.3 Material Characterizations

X-ray diffractometry (XRD) of the prepared powders were performed with specification using Cuk_1 radiation of wavelength (λ = 0.1548) with an operating working voltage as 40 kV. The scanning range for X-RD was fixed to 20-80˚ along with 6˚ min^{-1} scanning speed. For surface morphology analysis Scanning electron microscopy (SEM) was performed. Transmission electron microscopy (TEM, JEOL JEM-2100F) was employed with embedded EDS to further investigate the microstructural and grains under 200 kV accelerating voltage at room temperature. X-ray photoelectron spectroscopy (Escalab 250 Xi, Thermo Fisher Scientific, UK) was used to examine the surface properties of the YDG. Electrochemical impedance spectra (EIS) were measured in fuel cell conditions to investigate the electrocatalytic activities of the fabricated SOFC device by impedance analyzer (Gamry Reference 3000, Gamry Instruments, USA) at 550 ℃. The experimental data values os prepared sample are fitted using an equivalent circuit LRo(RctQct)(RmtQmt), where L is inductance of the instrument leads, R represents a resistance, and Q is the constant phase element (CPE) representing a non-ideal capacitor. In order to select the equivalent circuit, the deep analysis of EIS arcs corresponding to the ohmic and electrodes processes were evaluated. In each EIS curve, the intersection in the high frequency region and the corresponding real axis relates to the ohmic resistance (R_o). While the small arc at intermediate frequencies and the third process with a larger arc at low frequencies should be because of the charge transfer and mass transfer behaviors of electrode, respectively as reported in literature [1]. The fuel cell performance of as configured SOFC was determined by an electronic load instrument (IT8511, ITECH Electrical Co., Ltd., China) by using hydrogen as a fuel for HOR and open air as an oxidant for ORR catalytic performances.

2.4. First principle calculations using Density function theory (DFT)

The DFT calculations were done using the Quantum ATK Toolkit with supporting Material Studio and Vesta software. The Gd_2O_3 refined parameters i.e., metal ions (M-O) distances, cell volume were obtained from previous literature and Gd_2O_3 crystal structure was built in the Vesta software, while Y doped Gd_2O_3 crystal structure was constructed using Material studio software after successfully obtaining the Gd_2O_3 crystal structure. The generalized gradient approximation (GGA) and Perdew–Burke–Ernzerhof (PBE) exchange functional were used [2]. Spin polarized DFT + U theory calculations were employed on QUANTUM ATK TOOLKIT and ion-electron interactions were treated using projector augmented-wave potentials and GGA in the form of Perdew-Burke-Ernzerhof (PBE) and adopted to describe electron–electron interactions. For results accuracy, Electron wave functions were expanded using plane waves with an energy cut-off of 520 eV. For geometry optimization, all atoms of chosen samples were fully relaxed, and the convergence criteria for energy and force were set to 10^{-5} eV and 0.1 eV·nm^{-1}, respectively. Due to the well-known underestimation of band gap (E_g) in the GGA-PBE functional. Pseudo atomic calculations were performed considering according to the Gd and Y electronic configurations. Normally, k-points were set to be $5 \times 5 \times 5$ with MGGA exchange-correlation potential and the LBFGS optimizer method was set for geometry optimization with (1×10^{-4}) Hartree self-consistent field iteration and space group, Bravais lattice, and lattice factors were fully relaxed during YDG geometry optimization. Oxygen vacancy formation energy was calculated according to the following relation [3];

$$E_v = - E_{Total}\left(V_O^q\right) - E_{Total}(ideal) + \mu + q(E_F + E_{valan} + \Delta V) \quad (1)$$

where E_v is the oxygen vacancy formation energy, $E_{Total}\left(V_O^q\right)$ is the total energy of the defective superlattice with one oxygen vacancy. $E_{Total}(ideal)$ is the total energy of the ideal superlattice. The E_F is referenced to the Fermi level and E_{valan} is the valence-band maximum of the ideal superlattice.

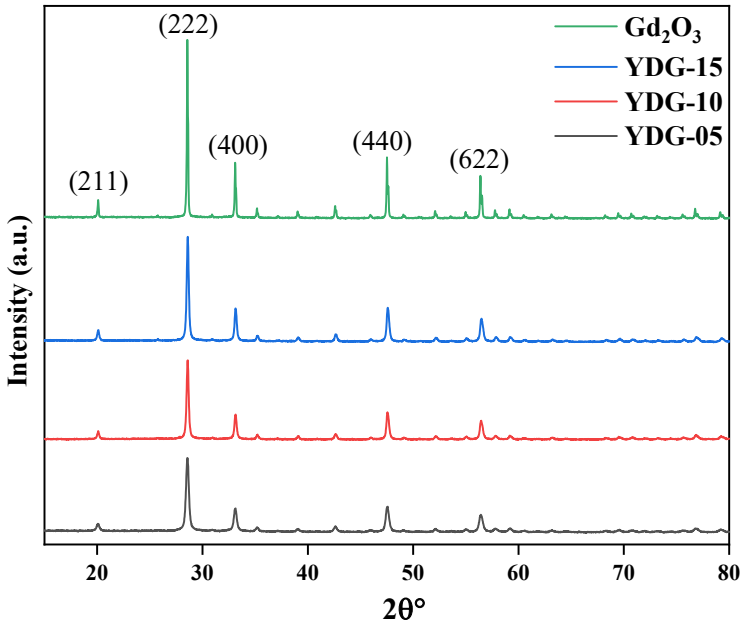

Fig.S1: XRD patterns of pure Gd_2O_3, YDG-05, YDG-10 (YDG) and YDF-15 samples

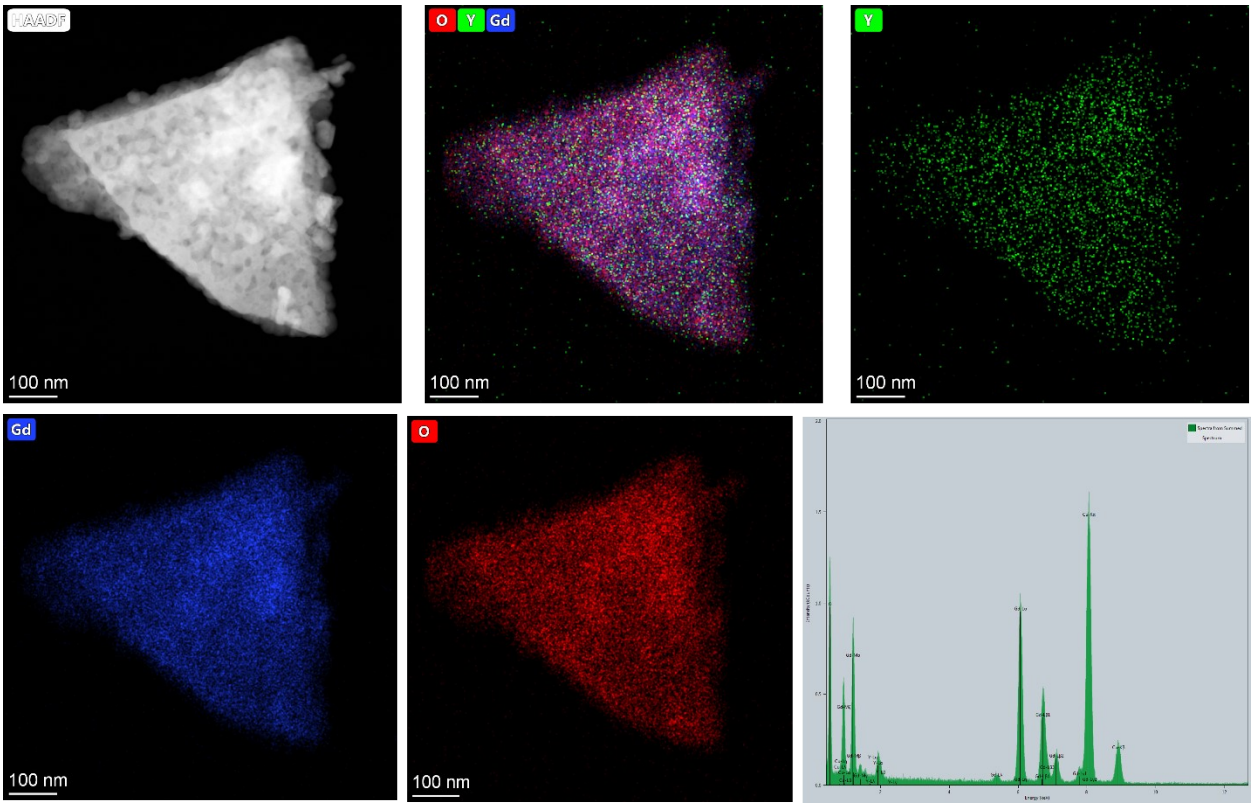

Fig. S2: Elemental mapping and EDS analysis of YDG sample.

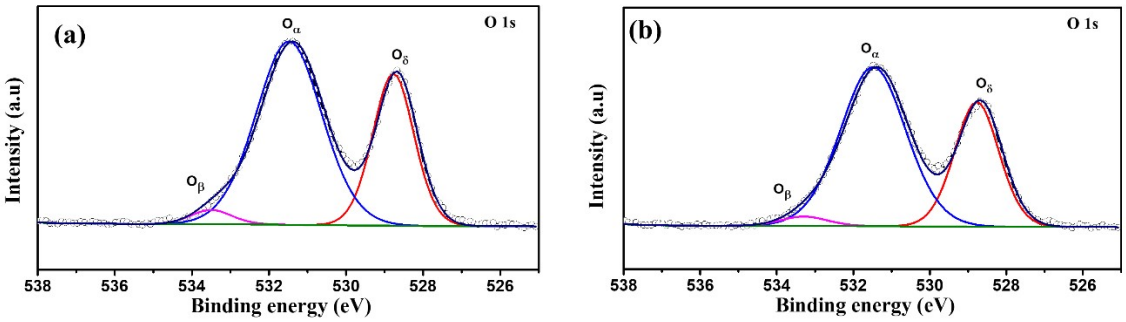

Fig. S3: (a-b) XPS O1s Spectra of 5% and 15% doping of $Y3^+$ in Gd_2O_3.

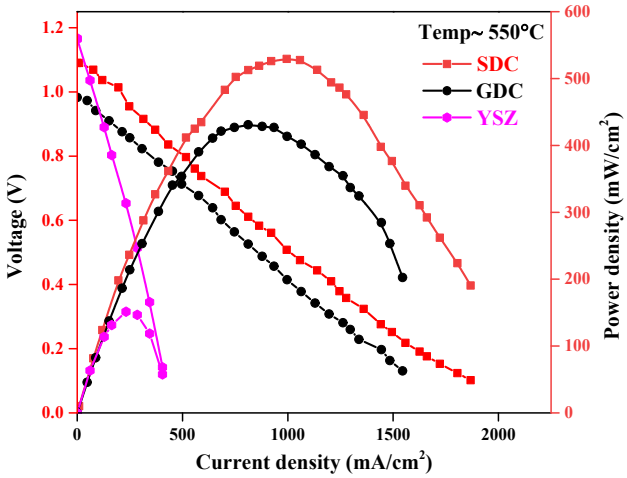

Fig. S4: I-V and I-P characteristics fabricated SDC, GDC and YSZ fuel cell devices at 550 ℃.

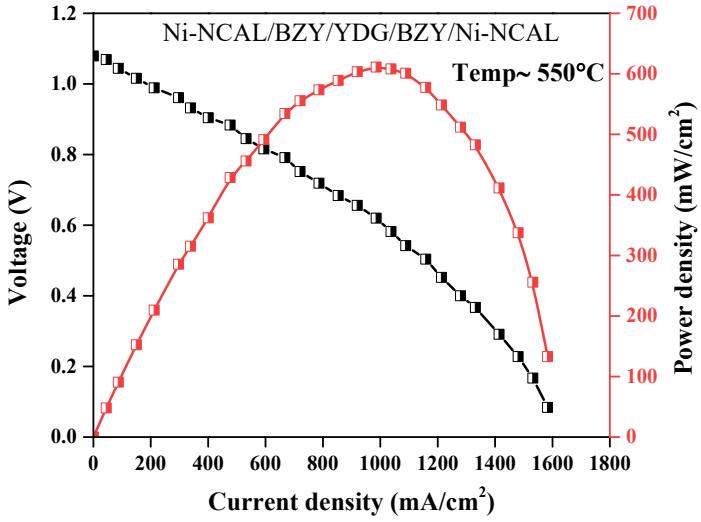

Fig. S5: Fuel cell performance with filter layer BZY with cell configuration Ni-NCAL/BZY/YDG/BZY/Ni-NCAL fuel cell device.

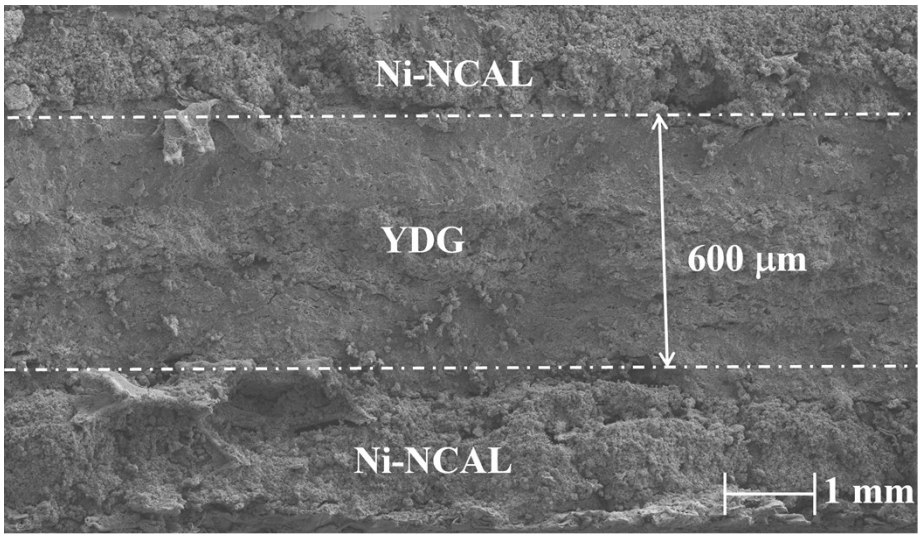

Fig. S6: SEM Cross-section image of Ni-NCAL/YDG/Ni-NCAL fuel cell device.

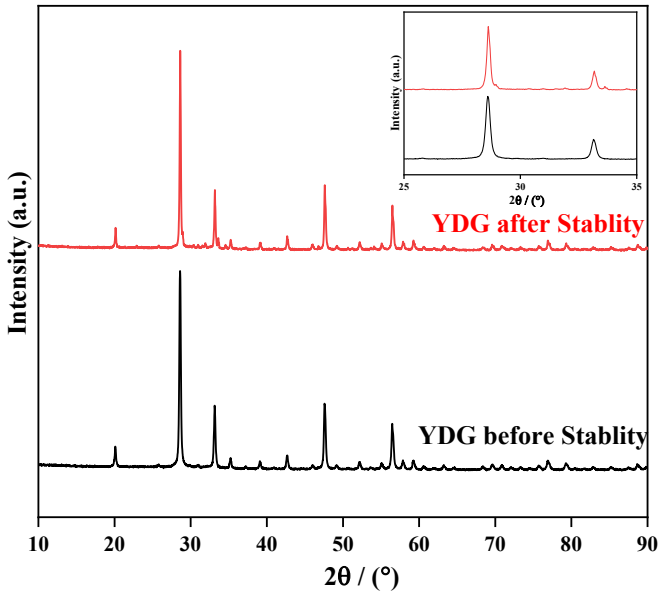

Fig S7. XRD analysis of YDG sample before and after durability measurements.

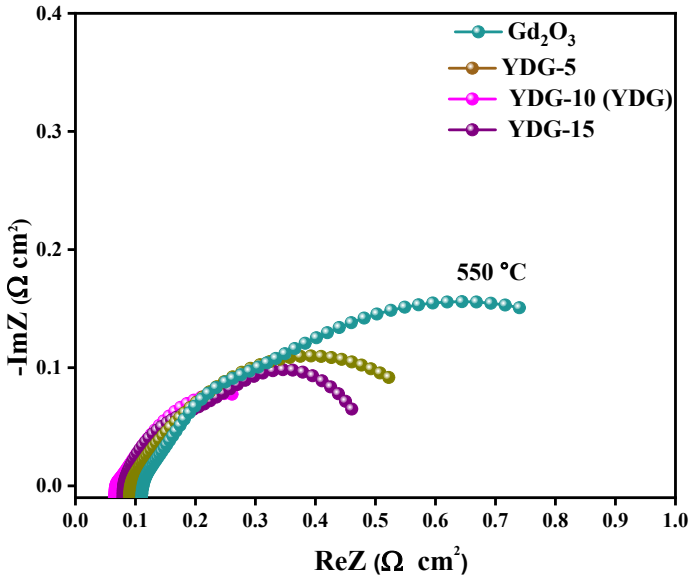

Fig. S8. EIS analysis of pure Gd_2O_3, YDG-05, YDG-10 and YDG-15 samples under H_2/air at 550 °C.

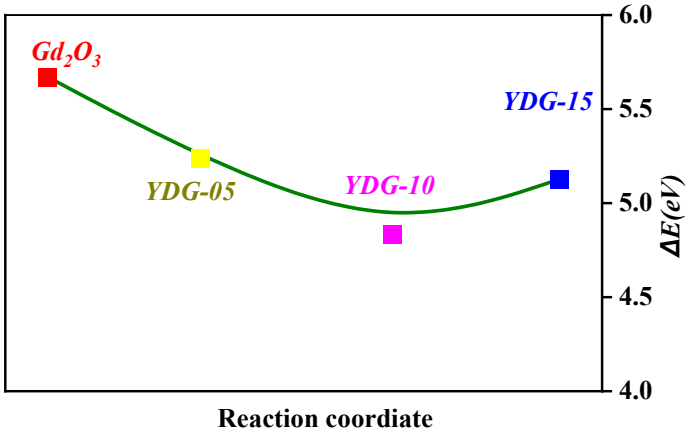

Fig. S9: Oxygen formation energies of pure Gd_2O_3, YDG-05, YDG-10 and YDG-15 samples using DFT calculations.

Table S1: EIS parameters of Ni-NCAL/YDG/Ni-NCAL fuel cell device.

Temperature (℃)	R_o	R_{ct}	Q_{ct}	N_1	C_1	R_{mt}	Q_{mt}	N_2	C_2	R_p
550	0.06	0.03	0.22	0.8	0.0627	0.17	3.2	0.5	1.74	0.2
520	0.07	0.04	0.42	0.8	0.1512	0.22	2.5	0.69	1.91	0.26
490	0.08	0.05	0.28	0.9	0.1721	0.33	2.8	0.8	2.74	0.38
460	0.09	0.13	1.8	0.7	0.9659	0.87	1.10E+00	0.88	1.09	1

Table S2: XPS simulated parameters for O1s Spectra of 5%, 10% and 15% doping of $Y3^+$ in Gd_2O_3

Composition	Peaks	Peaks BE	FWHM eV	Area (p) CPS.eV	Atomic %
5%Y doping of Y	O_δ	528.67	1.26	70744	34.00
	O_α	531.38	2.01	136728	62.91
	O_β	533.40	1.25	6595	3.09
10%Y doping of Y	O_δ	528.68	1.37	49324	30.76
	O_α	531.39	2.01	92811	66.65
	O_β	533.19	1.40	3771	2.59
15%Y doping of y	O_δ	528.69	1.29	59212	34.57
	O_α	531.53	2.01	115350	61.59
	O_β	533.01	1.32	6972	3.84

References

[1] Qiao, Zheng, Chen Xia, Yixiao Cai, Muhammad Afzal, Hao Wang, Jinli Qiao, and Bin Zhu. "Electrochemical and electrical properties of doped CeO2-ZnO composite for low-temperature solid oxide fuel cell applications." *Journal of Power Sources* 392 (2018): 33-40.

[2] Elstner, M., et al., Self-consistent-charge density-functional tight-binding method for simulations of complex materials properties. Physical Review B, 1998. 58(11): p. 7260.

[3] Mushtaq, N., Lu, Y., Xia, C., Dong, W., Wang, B., Shah, M. Y., ... & Zhu, B. (2021). Promoted electrocatalytic activity and ionic transport simultaneously in dual functional Ba0. 5Sr0. 5Fe0. 8Sb0. 2O3-δ-Sm0. 2Ce0. 8O2-δ heterostructure. *Applied Catalysis B: Environmental*, *298*, 120503.